Schottky electroluminescent diodes with n-doped germanium

M. Prost, M. El Kurdi, A. Ghrib, X. Checoury, N. Zerounian, F. Aniel, G. Beaudoin, I. Sagnes, C. Baudot, F. Boeuf , and P. Boucaud

Citation: Applied Physics Letters **104**, 241104 (2014); doi: 10.1063/1.4883466
View online: http://dx.doi.org/10.1063/1.4883466
View Table of Contents: http://scitation.aip.org/content/aip/journal/apl/104/24?ver=pdfcov
Published by the AIP Publishing

Articles you may be interested in
Schottky barrier height extraction from forward current-voltage characteristics of non-ideal diodes with high series resistance
Appl. Phys. Lett. **102**, 042110 (2013); 10.1063/1.4789989

Enhanced electroluminescence from the fluorine-plasma implanted Ni/Au-AlGaN/GaN Schottky diode
Appl. Phys. Lett. **99**, 062101 (2011); 10.1063/1.3622643

Strained Pt Schottky diodes on n -type Si and Ge
Appl. Phys. Lett. **88**, 143509 (2006); 10.1063/1.2191831

Electrical characterization of phosphorus-doped n-type homoepitaxial diamond layers by Schottky barrier diodes
Appl. Phys. Lett. **84**, 2349 (2004); 10.1063/1.1695206

Visible and infrared rare-earth-activated electroluminescence from indium tin oxide Schottky diodes to GaN:Er on Si
Appl. Phys. Lett. **74**, 182 (1999); 10.1063/1.123286

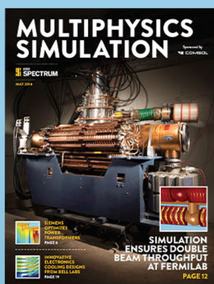

Free online magazine
MULTIPHYSICS SIMULATION
READ NOW

This article is copyrighted as indicated in the article. Reuse of AIP content is subject to the terms at: http://scitation.aip.org/termsconditions. Downloaded to IP: 129.175.97.14 On: Mon, 16 Jun 2014 14:18:44

Schottky electroluminescent diodes with n-doped germanium

M. Prost,[1,2] M. El Kurdi,[1] A. Ghrib,[1] X. Checoury,[1] N. Zerounian,[1] F. Aniel,[1] G. Beaudoin,[3] I. Sagnes,[3] C. Baudot,[2] F. Boeuf,[2] and P. Boucaud[1,a)]
[1]*Institut d'Electronique Fondamentale, CNRS-Univ. Paris Sud 11, Bâtiment 220, F-91405 Orsay, France*
[2]*STMicroelectronics, 850 Rue Jean Monnet, F-38920 Crolles, France*
[3]*Laboratoire de Photonique et de Nanostructures, CNRS - UPR 20, Route de Nozay, F-91460 Marcoussis, France*

(Received 29 April 2014; accepted 2 June 2014; published online 16 June 2014)

n-doped germanium can be used as an active material for the realization of an optical source under electrical pumping. We propose to use Schottky contacts for germanium electroluminescent devices, and we show that carrier injection and electroluminescence in these Schottky devices can be optimized by depositing a thin Al_2O_3 interfacial layer on top of n-doped germanium. In the latter case, hole injection is optimized due to the drastic decrease of interface trap densities and room-temperature electroluminescence can be observed at small current injection with a higher differential efficiency as compared to the standard Schottky sample. © *2014 AIP Publishing LLC*. [http://dx.doi.org/10.1063/1.4883466]

The interest for germanium has significantly increased over the past years. Germanium can be used for the growth of multiple junctions III-V/Ge solar cells, as a channel material with high intrinsic carrier mobility for advanced Si complementary metal oxide semiconductor architectures or photodetection at telecom wavelength. n-doped germanium under tensile strain has also been proposed as an active material to realize an optical source for silicon photonics.[1] Germanium is thus becoming a key material for microelectronics or optoelectronics, and its use is enabled by the engineering between group IV materials or by growing heterostructures combining III-V and group IV materials.

For the Ge-based solar cells, the electroluminescent diodes, or the germanium laser, a significant effort is devoted to the optimization of the electrical injection or carrier collection. This has led to the study of the Fermi level pinning at the metal-Ge interface by many groups.[2–5] In the case of the germanium laser or electroluminescent devices,[6] an additional constraint is due to the fact that the carrier recombination must occur in heavily n-doped germanium.[7–9] Electroluminescence of p-n Ge diodes has already been reported by several groups.[10–16] For electrical devices, one critical step is the management of defect interface states which can severely affect the transport properties and the carrier injection through the interfaces. For electroluminescence with n-doped germanium, the blocking of hole injection can strongly limit the radiative recombination. The improvement of the interfacial state density is thus a major issue.

In this work, we have investigated electroluminescent devices with an active n-doped germanium region grown on an n-type substrate. We first propose to use a Schottky heterostructure to inject carriers in n-doped germanium. Electroluminescence can be observed at forward bias,[17] since minority carriers are also injected in the structure at large current.[18] We show that the deposition of a thin Al_2O_3 interfacial layer can drastically improve the carrier injection. Without this interfacial layer, the electroluminescence is only observed above a certain threshold that corresponds to the discontinuity measured in the I-V characteristic. We associate this kink to an undesirable potential barrier for hole injection. The kink can be suppressed either under optical pumping or by inserting an Al_2O_3 barrier. A smooth I-V curve is then obtained and room-temperature electroluminescence can be observed at any positive bias with a much larger efficiency.

The studied samples were fabricated in a metal-organic vapor phase epitaxy reactor that can handle both germanium and III–V elements.[9,19,20] As Ge and GaAs are nearly lattice-matched, this provides a high quality Ge layer without a defective region as the one present in Ge/Si heterostructures due to misfit dislocations. We use isobutylgermane as precursor for the germanium. The n-doped Ge layers are directly grown on an n-doped GaAs substrate (doping level of $10^{18}\,cm^{-3}$). The Ge thickness is 300 nm and its n-doping is around $1-1.5\times10^{19}\,cm^{-3}$.[21] The samples were processed into mesas with $20\times20\,\mu m^2$ typical dimensions. For electroluminescence measurements, a window opening at the center ($4\times15\,\mu m^2$) of the processed mesa was fabricated in order to collect the emitted light. A Ti/Au metal contact is then directly deposited on Ge (Ger302A) or by inserting an Al_2O_3 intermediate barrier (Ger302B) before depositing an Al/Au metal contact (200–500 nm thickness). It is well known that the Schottky barrier height for a metal/Ge interface has a very weak dependence on the metal work function. The Fermi level is pinned close to the charge neutrality level which is close to the germanium valence band.[2] The electron barrier height is thus close to the Ge band gap. The introduction of a thin tunnel barrier like Al_2O_3 allows the depinning of the Fermi level.[3] This interfacial layer can passivate the interface states and reduce the metal-induced gap states. We note that there are no general rules that can account for Schottky barrier heights at the metal-semiconductor interface without detailed knowledge of the interface.[22] The Al_2O_3 is only 1.2 nm thick in order to minimize the tunneling resistance.[5] The n-type GaAs substrate is used as contact layer,

a)URL: http://pages.ief.u-psud.fr/QDgroup. Electronic mail: philippe.boucaud@ief.u-psud.fr

© 2014 AIP Publishing LLC

This article is copyrighted as indicated in the article. Reuse of AIP content is subject to the terms at: http://scitation.aip.org/termsconditions. Downloaded to IP: 129.175.97.14 On: Mon, 16 Jun 2014 14:18:44

to provide low ohmic contact resistance and carrier confinement in germanium. The ohmic contact is formed by an Au/Ge/Ni/Au metal contact followed by a rapid thermal annealing, prior to the Schottky contact metallization on germanium to avoid interdiffusion.

Figure 1(a) shows the I-V characteristic of the standard Schottky without interface barrier (Ger302A) as a function of the temperature. In lightly doped semiconductor Schottky junction, the current is driven by thermionic emission where the carriers are thermally excited over the potential barrier. But in heavily doped semiconductors, the length of the space charge region formed by the Schottky barrier is very short. This allows carrier tunneling through the barrier, and the current is driven by field emission. A criterion allows one to estimate which type of transport is predominant, depending on the doping level, by evaluating the energy related to the tunneling probability.[23,24] In the present case, the energy related to the tunneling probability is close to the thermal energy, which indicates that the transport mechanism is a combination between the two contributions cited above, called the thermionic-field emission. This behavior is observed in the I-V measurements. The saturation current is

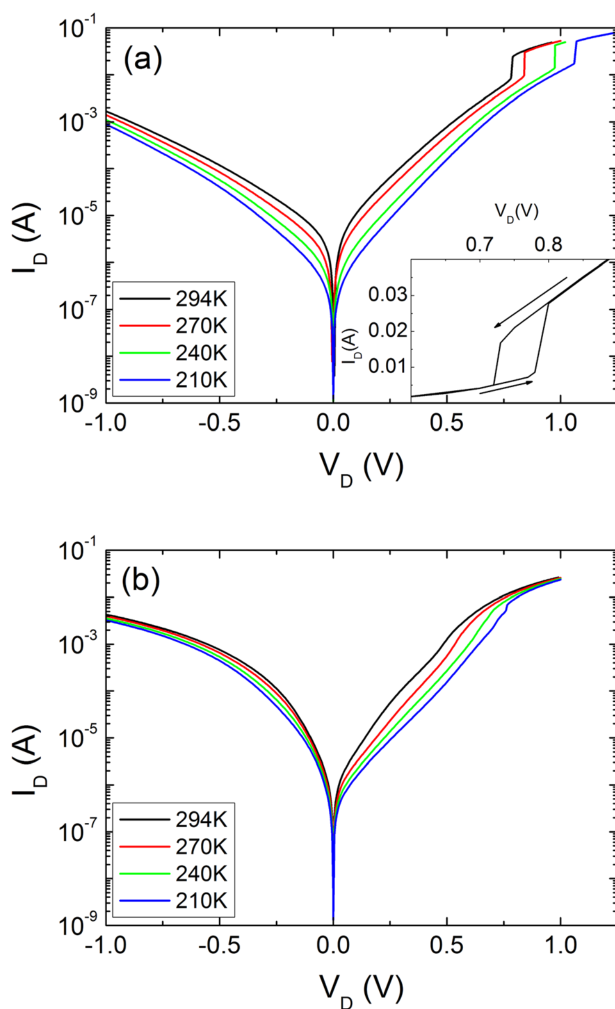

FIG. 1. (a) Current vs bias for the standard Schottky sample (Ger302A) as a function of temperature. The inset shows the hysteresis that occurs around the discontinuity. (b) I-V curve for the sample with the interfacial Al_2O_3 barrier (Ger302B) as a function of temperature. The surface is $20 \times 11\ \mu m^2$ and $24 \times 15\ \mu m^2$ for Ger302A and Ger302B, respectively.

weakly dependent on the temperature, which is characteristic of thermionic-field emission transport at the interface between the metal and the semiconductor. The striking feature in Fig. 1(a) is the kink for the current observed under forward bias. The abrupt change in current occurs at around 0.8 V at room temperature and the discontinuity value shifts to higher voltage as the temperature is decreased. In the discontinuity region, the current increases by a factor of 3 for a bias increase of 20 mV. It occurs for large current in the mA range corresponding to injected current densities in the kA cm^{-2} range. The curves presented in Figure 1 are obtained by a single sweep from 0 to large bias. The I-V curve corresponding to the first voltage sweep is usually slightly shifted before the system can be stabilized. When the voltage is decreased from high to low values, the I–V curve exhibits a strong hysteresis, with the abrupt change in the current occurring at a much lower bias (−0.2 V). This is shown in the inset of Fig. 1(a). The I–V curves are significantly different for the Schottky sample with the interfacial barrier (Ger302B) as shown in Fig. 1(b). The discontinuity disappears for temperatures down to 240 K and can only be slightly observed at 210 K. The Al_2O_3 barrier has thus suppressed the mechanisms that were blocking the current. At a fixed applied bias below the discontinuity, the injected current density is larger for the sample with the interfacial barrier. Similar behavior has also been observed with TiO_2 interfacial layers on n-germanium.[5] This is a consequence of Fermi-level depinning at the metal-semiconductor interface, the ultrathin insulator layer placed between the metal and the semiconductor leading to a lowering of the Schottky barrier height, and a stronger dependence on metals used.

In the following, we describe the electroluminescence results obtained at room temperature with the n-doped germanium Schottky samples grown on an n-type substrate. Figure 2(a) shows the room temperature electroluminescence spectra of the standard Schottky sample (Ger302A), while Fig. 2(b) shows the electroluminescence of the Schottky sample with the interfacial barrier (Ger302B). The electroluminescence spectrum is dominated by the direct band gap recombination observed around 1650 nm for the standard Schottky sample (Ger302A) and around 1570 nm for the Schottky sample with the interfacial layer (Ger302B).[25] The indirect band gap recombination is observed as a shoulder on the low energy side (long wavelength between 1800 and 2000 nm) of the spectrum. It first indicates that electroluminescence can be observed under forward bias by applying a Schottky contact on n-doped germanium. This represents a major simplification for the design of electroluminescent diodes. The observation of electroluminescence is a signature of minority carrier injection in the n-doped germanium active layer.[18] There are two major differences between the spectra in Figs. 2(a) and 2(b). The direct band gap recombination is resonantly peaked around 1650 nm for Ger302A, whereas the direct band gap recombination occurs around 1570 nm for Ger302B. For Ger302A, we can observe that the resonance peak first shifts to short wavelength as the current increases and then shifts to long wavelength at high current when thermal effects are present. For the Schottky sample with the Al_2O_3 barrier, only a red-shift is observed at high current densities due to thermal heating of the sample. As

This article is copyrighted as indicated in the article. Reuse of AIP content is subject to the terms at: http://scitation.aip.org/termsconditions. Downloaded to IP: 129.175.97.14 On: Mon, 16 Jun 2014 14:18:44

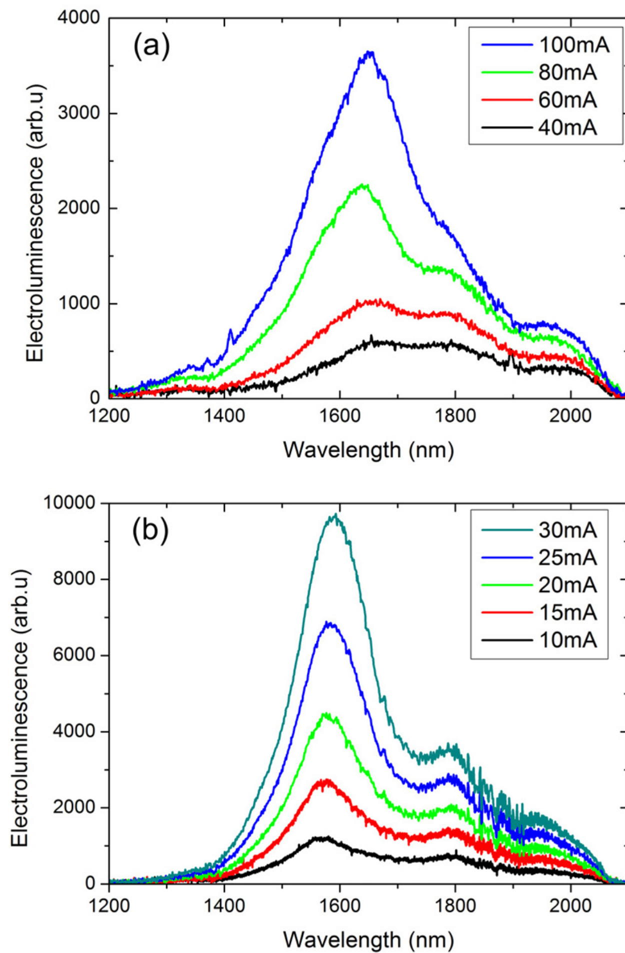

FIG. 2. (a) Room temperature electroluminescence for the standard Schottky sample (Ger302A) as a function of current. (b) Room temperature electroluminescence for the sample with the interfacial Al_2O_3 barrier (Ger302B) as a function of temperature. The vertical scale is different between figures (a) and (b). The electroluminescence amplitude for Ger302B is much larger for a reduced injected current. The diode areas are identical.

will be discussed below, we associate the difference of resonance wavelength of direct band gap recombinations between both samples (1570 nm vs 1650 nm) to the potential profile between the Schottky contact and the semiconductor. This results in spatially indirect radiative transitions for the Ger302A sample and leads to lowering recombination energy.[26] As the applied bias is increased, the separation between electrons and holes is decreased, thus reducing the spectral shift between the direct band gap recombinations. The spatially indirect transition also leads to a broadening of the recombination as observed in Fig. 2(a). The indirect band gap recombination (in k-space) is not significantly affected by this effect as it mostly stems from a zone far from the surface, whereas the direct band gap recombination is stronger close to the surface, as a consequence of reabsorption. The second main difference is that electroluminescence is only observed for an applied bias larger than the one corresponding to the I-V discontinuity, i.e., at large current densities. It is not the case for the sample with the interfacial barrier where electroluminescence is easily observed at smaller currents. This behavior is summarized in Fig. 3 that depicts the electroluminescence amplitude at peak maximum as a function of current density. The sample with the Al_2O_3 interfacial

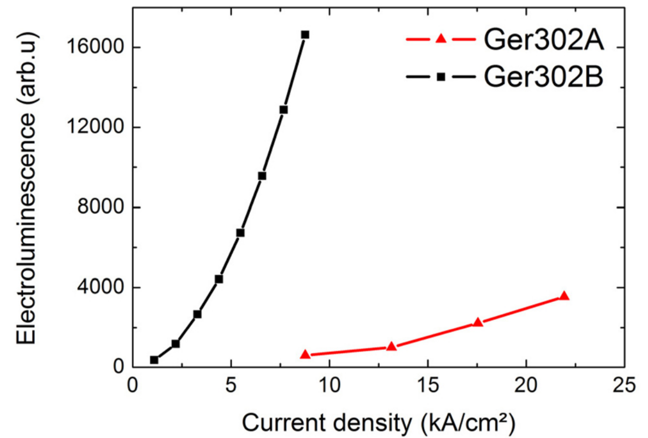

FIG. 3. Comparison of electroluminescence peak amplitude as a function of the injected current density for standard Schottky sample (triangle) or for the sample with the interfacial Al_2O_3 barrier (squares).

barrier exhibits significantly higher photoluminescence amplitude along with a significantly larger differential variation. It indicates that minority carrier injection, which is necessary to observe radiative recombinations, is much favored for sample Ger302B. Similar results were obtained for pulsed current injections. With a duty cycle of 10%, the amplitude of the measured electroluminescence is linear with the applied current up to 13 kA cm^{-2} without any redshift in the peak wavelength. The superlinear dependence shown in Fig. 3 is mainly due to heating effect, which is consistent with a redshift in the peak wavelength.[11]

The information brought by electroluminescence spectra is very complementary with the one obtained by standard I-V measurements. One can distinguish between majority and minority carrier injection, as holes are necessary to observe radiative recombination with n-doped layers. We have performed the same I–V measurements as reported in Fig. 1 under optical pumping. The striking feature is that the discontinuity in the I–V curve for the standard Schottky sample disappears under optical pumping for pump intensities larger than 3 W cm^{-2} at 632.8 nm. It indicates that the states, which are blocking the current injection, can be saturated under optical injection in the same way that they are quenched with the interfacial Al_2O_3 barrier. We thus propose the schematics band diagram shown in Fig. 4 to explain the

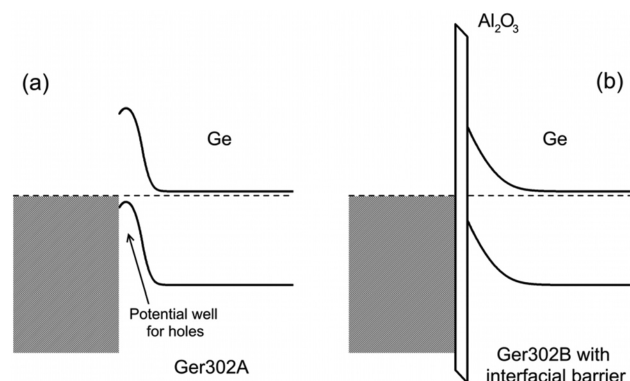

FIG. 4. Schematic band diagram for the standard Ger302A Schottky sample (a) and (b) for the sample with the interfacial Al_2O_3 barrier (Ger302B). The dashed line represents the Fermi level. The gray area represents the metal.

This article is copyrighted as indicated in the article. Reuse of AIP content is subject to the terms at: http://scitation.aip.org/termsconditions. Downloaded to IP: 129.175.97.14 On: Mon, 16 Jun 2014 14:18:44

experimental results. Fig. 4(a) shows the band diagram for the standard Schottky sample, while Fig. 4(b) shows the band diagram for the Schottky sample with the interfacial barrier. There is a breaking of the lattice periodicity at the semiconductor interface. It leads to the formation of interface states which are a mixture of acceptor-like conduction band states and donor-like valence band states.[2] For n-doped germanium, a large negative charge can be trapped at the interface. It can lead to the formation of a potential well for the hole minority carriers as well as a barrier potential for electron injection. The injected holes are preferably trapped in this potential, thus limiting the radiative recombination. As the current density increases, the well starts to be filled and at a critical value for the charge carrier concentration, there is a reduction of the potential barrier, which results in an abrupt increase of the current as observed in the I–V curve. This blocking barrier for minority carrier explains that no electroluminescence is observed below the I-V discontinuity for the standard Ger302A sample. It also explains the red-shift of the recombination as compared to photoluminescence, since spatially indirect recombination is likely to occur between holes trapped in the well and electrons in the n-doped layer. This band diagram is also consistent with the fact that the abrupt change in the I-V curve disappears when the measurements are performed under optical pumping. In the latter case, the minority photo-induced carriers can fill the potential well, thus decreasing the potential barrier height. Finally, this diagram is consistent with the hysteresis behavior observed with sample Ger302A. Once the potential well is filled, the injected current can remain large even for bias values below the threshold. This is achieved when the bias is swept from high to low values, up to the point where the potential well is depleted. Similar interface band diagram has also been observed in the case of GaInP/Ge sub-cells integrated in multi-junction solar cells.[27] We note that the two band diagrams presented in Fig. 4 are consistent with the metal-induced gap state theory originally introduced by Heine[28] and Tersoff's branch-point theory.[29] The insertion of the interfacial Al_2O_3 barrier suppresses or at least strongly diminishes the interfacial state density and the potential well for minority carriers, thus modifying the Fermi level pinning by the passivation of the dangling bonds of the semiconductor substrate as discussed in detail by Mönch.[30] It also lowers the potential barrier for electron injection. Consequently, there is no abrupt change in the current density vs. bias and the current density is larger for the same applied bias as compared to the standard Schottky sample. The injection of minority carrier is enhanced, thus explaining that electroluminescence can be observed at much lower current densities and with a higher differential efficiency. The depinning of the Fermi level by the interfacial layer is thus beneficial for both electron and hole carrier injection. Further investigations based, for example, on *ab initio* calculations would be required in order to accurately describe the changes at the interfaces.[22]

In conclusion, we have shown that room-temperature electroluminescence can be obtained under forward bias with Schottky contacts on n-doped germanium grown on an n-type substrate. The insertion of a thin Al_2O_3 interfacial layer can drastically improve the carrier injection. It suppresses the abrupt change in the I-V curve and allows one to observe electroluminescence at much smaller current injection with a higher differential efficiency. We have explained the observed properties by the formation of a potential well for minority carriers in the case of the standard Schottky sample. This barrier is suppressed by introducing the thin interfacial layer. We expect that these results will have an impact for the design of germanium-based emitters for silicon photonics. These results also indicate that valuable information can be obtained on metal/germanium interface by combining standard electrical measurements with room-temperature electroluminescence measurements.

This work was supported by Agence Nationale de la Recherche under GRAAL convention (ANR 2011 B S03 004 01) and by "Triangle de la Physique" under Gerlas convention. This work was also partly supported by the RENATECH network and by Région Ile de France (C'Nano2011-Nanoetch project). M. Prost was funded by a CIFRE Grant.

[1] J. Liu, X. Sun, D. Pan, X. Wang, L. C. Kimerling, T. L. Koch, and J. Michel, Opt. Express **15**, 11272–11277 (2007).
[2] A. Dimoulas, P. Tsipas, A. Sotiropoulos, and E. K. Evangelou, Appl. Phys. Lett. **89**, 252110 (2006).
[3] Y. Zhou, M. Ogawa, X. Han, and K. L. Wang, Appl. Phys. Lett. **93**, 202105 (2008).
[4] T. Nishimura, K. Kita, and A. Toriumi, Appl. Phys. Express **1**, 051406 (2008).
[5] J. -Y. J. Lin, A. M. Roy, A. Nainani, Y. Sun, and K. C. Saraswat, Appl. Phys. Lett. **98**, 092113 (2011).
[6] R. E. Camacho-Aguilera, Y. Cai, N. Patel, J. T. Bessette, M. Romagnoli, L. C. Kimerling, and J. Michel, Opt. Express **20**, 11316–11320 (2012).
[7] B. Dutt, D. Sukhdeo, D. Nam, B. Vulovic, Z. Yuan, and K. Saraswat, IEEE Photon. J. **4**, 2002–2009 (2012).
[8] M. El Kurdi, T. Kociniewski, T.-P. Ngo, J. Boulmer, D. Debarre, P. Boucaud, J. F. Damlencourt, O. Kermarrec, and D. Bensahel, Appl. Phys. Lett. **94**, 191107 (2009).
[9] M. de Kersauson, M. El Kurdi, S. David, X. Checoury, G. Fishman, S. Sauvage, R. Jakomin, G. Beaudoin, I. Sagnes, and P. Boucaud, Opt. Express **19**, 17925–17934 (2011).
[10] X. Sun, J. Liu, L. C. Kimerling, and J. Michel, Appl. Phys. Lett. **95**, 011911 (2009).
[11] S.-L. Cheng, J. Lu, G. Shambat, H.-Y. Yu, K. Saraswat, J. Vuckovic, and Y. Nishi, Opt. Express **17**, 10019–10024 (2009).
[12] M. de Kersauson, R. Jakomin, M. El Kurdi, G. Beaudoin, N. Zerounian, F. Aniel, S. Sauvage, I. Sagnes, and P. Boucaud, J. Appl. Phys. **108**, 023105 (2010).
[13] T.-H. Cheng, C.-Y. Ko, C.-Y. Chen, K.-L. Peng, G.-L. Luo, C. W. Liu, and H.-H. Tseng, Appl. Phys. Lett. **96**, 091105 (2010).
[14] D. Nam, D. Sukhdeo, S.-L. Cheng, A. Roy, K. C.-Y. Huang, M. Brongersma, Y. Nishi, and K. Saraswat, Appl. Phys. Lett. **100**, 131112 (2012).
[15] M. Oehme, M. Gollhofer, D. Widmann, M. Schmid, M. Kaschel, E. Kasper, and J. Schulze, Opt. Express **21**, 2206–2211 (2013).
[16] M. Kaschel, M. Schmid, M. Gollhofer, J. Werner, M. Oehme, and J. Schulze, Solid-State Electron. **83**, 87–91 (2013).
[17] A. Babinski, P. Witczak, A. Twardowski, and J. M. Baranowski, Appl. Phys. Lett. **78**, 3992–3994 (2001).
[18] W. Ng, S. Liang, and C. T. Salama, Solid-State Electron. **33**, 39–46 (1990).
[19] R. Jakomin, M. de Kersauson, M. El Kurdi, L. Largeau, O. Mauguin, G. Beaudoin, S. Sauvage, R. Ossikovski, G. Ndong, M. Chaigneau, I. Sagnes, and P. Boucaud, Appl. Phys. Lett. **98**, 091901 (2011).
[20] M. de Kersauson, M. Prost, A. Ghrib, M. El Kurdi, S. Sauvage, G. Beaudoin, L. Largeau, O. Mauguin, R. Jakomin, I. Sagnes, G. Ndong, M. Chaigneau, R. Ossikovski, and P. Boucaud, J. Appl. Phys. **113**, 183508 (2013).
[21] A. Ghrib, M. El Kurdi, M. de Kersauson, M. Prost, S. Sauvage, X. Checoury, G. Beaudoin, I. Sagnes, and P. Boucaud, Appl. Phys. Lett. **102**, 221112 (2013).
[22] R. T. Tung, Appl. Phys. Rev. **1**, 011304 (2014).
[23] F. Padovani and R. Stratton, Solid-State Electron. **9**, 695–707 (1966).
[24] A. Firrincieli, K. Martens, E. Simoen, C. Claeys, and J. Kittl, Microelectron. Eng. **106**, 129–131 (2013).

This article is copyrighted as indicated in the article. Reuse of AIP content is subject to the terms at: http://scitation.aip.org/termsconditions. Downloaded to IP: 129.175.97.14 On: Mon, 16 Jun 2014 14:18:44

[25]M. El Kurdi, H. Bertin, E. Martincic, M. de Kersauson, G. Fishman, S. Sauvage, A. Bosseboeuf, and P. Boucaud, Appl. Phys. Lett. **96**, 041909 (2010).
[26]P. Boucaud, S. Sauvage, M. El Kurdi, E. Mercier, T. Brunhes, V. Le Thanh, D. Bouchier, O. Kermarrec, Y. Campidelli, and D. Bensahel, Phys. Rev. B **64**, 155310 (2001).
[27]A. S. Gudovskikh, K. S. Zelentsov, N. A. Kalyuzhnyy, V. V. Evstropov, V. M. Lantratov, and S. A. Mintairov, J. Phys. D: Appl. Phys. **45**, 495305 (2012).
[28]V. Heine, Phys. Rev. **138**, A1689–A1696 (1965).
[29]J. Tersoff, Phys. Rev. Lett. **52**, 465–468 (1984).
[30]W. Mönch, J. Appl. Phys. **111**, 073706 (2012).

This article is copyrighted as indicated in the article. Reuse of AIP content is subject to the terms at: http://scitation.aip.org/termsconditions. Downloaded to IP: 129.175.97.14 On: Mon, 16 Jun 2014 14:18:44